Contrast-enhanced Coded Phase-inversion Harmonic Sonography of Knee Synovitis Correlates with Histological Vessel Density: 2 Automated Digital Quantifications

MARIE-JOËLLE KAISER, JEAN-PHILIPPE HAUZEUR, SILVIA BLACHER, JEAN-MICHEL FOIDART, MANUEL DEPREZ, ALEXANDRA ROSSKNECHT, and MICHEL G. MALAISE

ABSTRACT. ***Objective.*** To use contrast-enhanced coded phase-inversion harmonic B-mode sonography to assess the acoustic enhancement of the synovial area of the knee; and to compare the data with the histological vessel density.

Methods. Eleven patients eligible for a knee arthroscopy were studied. Acoustic quantification was carried out by a digital image analysis program that detects the time-dependent increase [intensity (time) = k × time + C] of gray-level intensity in all the pixels of a specific region of interest (ROI) following intravenous injection of the microbubble contrast agent sulfur hexafluoride. Echo-guided synovial biopsies were carried out in the same ROI. Synovial vessel areas were quantified after Factor VIII immunostaining of synovial biopsies using an automated digital image analysis.

Results. Significant ($p < 0.05$) correlations were observed between histological vessel density and percentage of the synovial area with a k value > 0.01 ($r = 0.93$) and k_{max} values ($r = 0.79$), as well as between the 2 latter parameters ($r = 0.72$). The histological vessel density and the 2 acoustic parameters were also significantly correlated with the logarithm of erythrocyte sedimentation rate ($r = 0.77$, $r = 0.87$, $r = 0.67$, respectively) and with log C-reactive protein serum concentration ($r = 0.69$, $r = 0.83$, $r = 0.62$, respectively).

Conclusion. Contrast-enhanced coded phase-inversion harmonic B-mode sonography coupled with an appropriate data analysis method is a new tool to identify and quantify vessel density in knee synovitis. (First Release April 15 2009; J Rheumatol 2009;36:1391–400; doi:10.3899/jrheum.080584)

Key Indexing Terms:
DIGITAL IMAGE ANALYSIS SYNOVIAL VASCULARIZATION
CODED PHASE-INVERSION HARMONIC B-MODE SONOGRAPHY
MICROBUBBLE CONTRAST SONOGRAPHY ARTHROSCOPY HISTOLOGY

In addition to synovial membrane proliferation and massive leukocytic infiltrate, neovascularization is a characteristic of the pannus of rheumatoid arthritis (RA). Identification and quantification of the effusion and of the synovitis can now be addressed through application of high resolution B-mode ultrasonography (US) to joints in RA[1-4] or osteoarthritis (OA)[5,6]. With synovial thickening, the vascularization is a condition associated with the destructive capacity of the RA pannus[7,8]. Visualization and possibly quantification of angiogenesis, now considered crucial in RA[9], can be obtained with color[10-16] and power Doppler[3,17-33] sonography. The power Doppler technique, more sensitive than color Doppler[17,19], has been correlated with the histological assessment of synovial membrane microvascular density in knee[24] and hip[27] joints of patients with OA and RA. Briefly, in rheumatoid joints, the presence of a Doppler signal was observed in 23% of hands and knees positive at sonography[31], in 40%[25] to 54%[29] of swollen and/or tender metacarpophalangeal (MCP) joints, 50% of knees[34], 52% of MCP and proximal interphalangeal (PIP) joints, and in 60% of wrists and both swollen and tender MCP and PIP joints[14]. Quantification of Doppler images has been performed using semiquantification scales[3,11,13,18,21,22,24,27,30] or computer-aided image analysis[10,12,14,24,27,32]. Abnormalities in

From the Department of Rheumatology, GIGA Research, CHU Liège; Laboratory of Tumor and Development Biology; and Department of Pathology, CHU Liège, University of Liège, Liège, Belgium; and GE Healthcare Technologies, Ultrasound Europe, Solingen, Germany.

Supported by the Fond d'investissement pour la recherche scientifique (FIRS), University Hospital Liège, Liège, Belgium.

Dr. Kaiser and Dr. Hauzeur contributed equally to this work.

M-J. Kaiser, MD; J-P. Hauzeur, MD, PhD; M.G. Malaise, MD, PhD, Department of Rheumatology, GIGA Research, CHU Liège; S. Blacher, PhD; J-M. Foidart, MD, PhD, Laboratory of Tumor and Development Biology; M. Deprez, MD, PhD, Department of Pathology, CHU Liège, University of Liège; A. Rossknecht, PhD, GE Healthcare Technologies, Ultrasound Europe.

Address correspondence to Dr. M.G. Malaise, Department of Rheumatology, University Hospital Liège, B4000 Liège, Belgium. E-mail: Michel.Malaise@ulg.ac.be

Accepted for publication November 28, 2008.

Doppler sonography of inflamed joints have also been shown to reduce or to normalize after steroid injections of joints[15,18,21] or administration of etanercept[12] and infliximab[3,32].

Power Doppler US as a technique remains limited in the detection of slow flow and flow in small vessels[13], and signal interpretation remains delicate, mainly limited by flash artifacts and variability generated by machine settings, the operator, and the acoustic conditions[35]. Recent reports have examined these difficulties and limitations[36-38].

The use of microbubble contrast agent is another US approach in assessment of vascularization[39], as injection of microbubbles of galactose/palmitic acid (Levovist®; Schering AG, Berlin, Germany) enhances both gray-scale images and flow-mediated color[13,16] and power[23,26,28,29,33] Doppler signals, increasing US sensitivity in most studies. The number of positive MCP and PIP joints rose from 58% to 78%[13] with color Doppler, and increased the power Doppler signal score in 72% of knees in a study[28] using semiquantitative scales. A recent study[34] described that the percentage of tender and swollen RA joints showing a power Doppler signal rose from 50% to 80% after perfusion of a second-generation microbubble contrast agent such as SonoVue® (Bracco, Milan, Italy), an aqueous suspension of sulfur hexafluoride microbubbles[40]. Lastly, a quantification method has been proposed measuring the area of the underlying time-intensity curve recorded within 5 minutes after injection of the microbubble agent[26]; this measure was significantly reduced after one intraarticular steroid injection in the knee[33]. Because limitations such as blooming artifacts, poor spatial resolution, and low sensitivity to slow flow remain[41], it was of interest to develop another approach.

Applied to study of the liver for diagnosis of metastases or hepatocellular carcinoma[39,41], coded phase-inversion (CPI) harmonic US depicts signal from microbubbles with good accuracy and with spatial resolution devoid of Doppler-related artifacts[41]. Real-time continuous imaging in the early arterial phase, i.e., 15–40 seconds after intravenous injection of microbubble contrast agent, provides enhanced signal intensity indicating the presence of microbubbles in tumor vessels of the metastasis[39] or hepatocellular carcinoma[41], identifying the tumor neovascularization. Our aim was to evaluate whether the technique could be applied to *in vivo* quantification of synovial vascularization. To achieve this, an original computation program was developed; results were compared to the "gold standard" for vessel identification, an immunohistological image analysis quantification on synovial biopsies collected from the corresponding region of interest (ROI) where US measurements were performed. US and histological data were then compared to the biological signs of inflammation, the erythrocyte sedimentation rate (ESR), and the serum C-reactive protein (CRP) concentration.

MATERIALS AND METHODS

Study population. After approval by the ethical committee of the university hospital of Liège and with informed consent, 11 patients were prospectively enrolled to undergo a knee synovial biopsy during arthroscopy for diagnostic (4 cases) or therapeutic (joint lavage in 1, synovectomy in 6 cases) purposes. Seven patients had RA, 3 had psoriatic arthritis (PsA), and 1 OA. Epidemiological data (age, sex, disease duration, ESR and CRP) are given in Table 1.

Procedures. US and arthroscopy were carried out at the same time by 2 rheumatologists (JPH and MJK) experienced in arthroscopy and musculoskeletal sonography. Under local (n = 4), spinal (n = 4), or general anesthesia (n = 3), an arthroscope (2.7 or 4 mm diameters) was inserted anterolaterally and a biopsy forceps was placed by the superolateral portal. No tourniquet and no adrenaline were used to avoid any modification of the local vascularity. The US study was performed before any fluid distension of the joint.

Ultrasound evaluation. The US evaluation was performed with a GE Logiq 9 device (GE Healthcare Technologies, Milwaukee, WI, USA) using a linear 7-MHz transducer. The ROI was the superomedial recess of the quadricipital pouch because it is generally rich in synovitis and easy to access for biopsy from the superolateral approach (Figure 2A). The US contrast agent used was SonoVue® (Bracco), an aqueous suspension of sulfur hexafluoride microbubbles[36]. This blood-pool Doppler enhancing agent is known to be well tolerated, with a good safety profile[40,42]. At time zero, a 5-ml intravenous bolus (8 μl sulfur hexafluoride in microbubbles/ml) was rapidly injected manually through a 20-gauge cannula inserted into an antecubital vein, followed by a flush with 10 ml of sodium chloride 0.9%. No side effects were observed. The probe was stabilized on the same position.

The US program for image acquisition was the CPI harmonic program, a contrast agent-specific technique[37] that produces strong preferential imaging of the microbubbles in an image. The program encodes the transmitted signal with multiple frequencies to enhance the bubble resonance and decodes the received signal to process only the contrast harmonic signal and not the tissue harmonic signal. Briefly, 2 identical pulses with reverse polarity are transmitted to the tissue in rapid succession and the scanner detects and sums the echoes generated. Linear scattering from tissue results in a signal void, while nonlinear signals from microbubbles stand out[37]. Additionally, the CPI technique is used for good separation of the harmonic signal. This technique enhances the contrast-tissue ratio, the signal-noise ratio, and the penetration[37]. Video loops were recorded continuously during 2 minutes after the injection of microbubble agent and were recorded on the hard disk.

Biopsy procedure. Just after the US contrast test, a synovial biopsy was done at the same location as US acquisition (Figure 2A, 2B).

Immunohistochemistry. Each synovial specimen was analyzed *in toto* (8 to 20 sections). Sections (thickness 5 μm) were cut at 40 μm intervals from formalin-fixed, paraffin-embedded synovial tissue samples. Sections were dehydrated through graded alcohols, incubated in H_2O_2 (0.3 % for 15 min), and rinsed in distilled water followed by Tris buffer, pH 7.14, for 5 min. Factor VIII immunostaining was performed to identify blood vessels[43]. Sections were incubated with rabbit polyclonal antibody anti-human von Willebrand Factor VIII (1:100; code N1505, Dako, Glostrup, Denmark) for 1 h at room temperature. After 3 washes in Tris buffer (5 min), sections were incubated with Envision anti-rabbit secondary antibody (code K4011, Dako) for 30 min at room temperature and then washed again in Tris buffer (3 × 5 min). Immunoreactivity was visualized with 3,3'diaminobenzidine (DAB+, code K3468, Dako). Negative controls were obtained by omitting the primary antibody. Microphotographs were taken with a Zeiss Axioplan light microscope. At magnification 50×, the surface of the photographed field is 1.7 mm (L) x 1.18 mm (l) = 2 mm^2.

Digital image analysis. Image treatments for both US and histological sections were analyzed using Matlab software and Aphelion 3.2 software (Adcis, Herouville Saint-Clair, France). Algorithms developed in this work

Table 1. Population epidemiology, histologic vessel density, and sonographic parameters.

Patient	Epidemiology						Experimental Procedures			
							Histology		Ultrasonography	
	Age, yrs	Sex	Disease	Disease Duration, yrs	ESR, mm/h	CRP mg/l	Sections, (n)	Vessel Density* (% of ROI area)	k > 0.01 (% of ROI area)	k_{max}
1	61	M	RA	1	19	10	18	4.3 ± 2.2	47.9	8.4
2	33	M	RA	5	87	66	14	6.0 ± 1.2	53.3	7.5
3	68	F	RA	2	58	67	9	7.7 ± 2.1	54.1	13.4
4	28	F	RA	6	12	3	20	6.1 ± 1.4	50.7	7.1
5	59	M	RA	18	17	7	20	3.0 ± 1.6	46.3	5.1
6	75	F	RA	3	14	15	10	2.1 ± 0.6	46.6	6.3
7	61	F	RA	7	41	38	20	7.3 ± 1.3	51.6	9.3
8	48	M	PsA	12	10	2	10	3.1 ± 1.8	43.9	8.7
9	43	M	PsA	3	24	15	8	4.1 ± 1.2	47.2	7.1
10	28	M	PsA	1	2	1	9	2.0 ± 0.8	41.7	3.9
11	53	M	OA	2	7	3	20	1.4 ± 0.5	41.1	5.5

* Mean value ± standard deviation. RA: rheumatoid arthritis; PsA: psoriatic arthritis; OA: osteoarthritis; ESR: erythrocyte sedimentation rate; CRP: C-reactive protein (0–6 mg/l); ROI: region of interest.

were carried out using standard means of signal processing and mathematical morphology[44-46].

Image processing of histological sections. The main preprocessing steps of histological sections we used are illustrated in Figure 1, as follows.

1. Images were recorded in the full-color red (Figure 1.2), green (Figure 1.3), and blue (RGB) (Figure 1.4) space. As the vessels appeared with greater contrast in the blue channel (Figure 1.4), the blue image was used for all subsequent analysis.

2. A mask was then created by applying a threshold transformation (Figure 1.5). Combination of the original image (Figure 1.4) with the mask (Figure 1.5) allowed isolation of the studied tissue from the background (Figure 1.6).

3. To enhance contrast of the vessels, a morphological filter, the so-called "top hat" operator[44], was applied on the masked image and the resulting image was subtracted from the previous one. In the resulting image (Figure 1.7), vessels appeared as black structures easily distinguished from the background.

4. The enhanced image was binarized with a threshold value computed automatically using the entropy of the gray-level histogram of the image[45,46]. After this, all pixels located in the tissue area were allocated a value of 1 and those located in the background a value of 0 (Figure 1.8).

5. A morphological filter ("opening" operator) was used to eliminate small objects and artifacts[44]. The lower limit of a vessel size was arbitrarily fixed to 5 pixels, corresponding to the limit of resolution of the optical microscope at the magnification used (Figure 1.9). For each binary image, the blood vessel density was determined as the number of pixels characteristic of a vessel divided by the number of pixels characteristic of the tissue.

6. Vessel density was expressed as the mean value of the densities of 8 to 20 images, the number of images processed depending upon the number of slices obtained, which is a function of the size of the biopsy sample (one density/image, one image/slice; Table 1).

Image processing of US images. The GE Logiq 9 device provides a file (AVI format) that contains a video stream. In our study, a typical AVI file had the following technical characteristics: size 93,605,888 bytes; 2281 images per video; 38 images/second during playback; image size 532 × 434 pixels; and type of image: true color (RGB).

Figure 2, A1 and A2, shows representative US images of the synovial region. Using software supplied with the GE Logiq 9 device, the time evolution of the gray-level intensity of 6 different manually chosen ROI can be selected (Figure 2, A3 and A4). As shown in Figure 2 A3, the gray level of 4 different ROI were recorded and remained stable with time in the absence of bubble contrast. By contrast, in the presence of bubble contrast agent, the gray level of one ROI (the yellow one, Figure 2 A4) abruptly increased 10 seconds after the beginning of the video stream, the time needed for the contrast agent to appear in the ROI, whereas the gray level of the other ROI (the green) remained unchanged in otherwise identical experimental conditions. As shown in Figure 2 A4, the software adjusts the gray level evolution with time with the equation: intensity (time) = $B + A(1 - e^{-kt})$.

This manual processing is slow, the manual positioning remains subjective, and the software does not allow probing a continuous region, but only 6 points. Therefore, in order to determine the contrast-enhanced acoustic density on the whole image obtained, we used an automated computer-assisted image analysis procedure, as follows.

1. Twenty images, one every 100 images (Figure 2 B1), were extracted from the video, this number corresponding to our available computing capacity.

2. Each image was restricted to a frame of 400 × 400 pixels. To allow automatic determination of the gray-level evolution of each point of the images (20 frames of 16,000 pixels), the frames were strictly stacked, taking the first one as reference (Figure 2 B2).

3. The gray-level intensity as a function of time for each pixel was determined in the 20 successive images.

4. Although it was best fitted with the exponential equation, we decided to adjust the evolution of the gray-level intensity with time, for each pixel of the image, with the more simple linear equation, Intensity (time) = k × time + C; Figure 2 A4.

5. The 160,000 (400 × 400) values of k, which describe the gray-level evolution of each point of the image, are represented in a color-graduated scale from its minimum value in blue (k = 0) to maximum value in red (Figure 2 B3).

6. As pixels with a k value of 0 do not exhibit acoustic enhancement, we postulated that those with a k value different from zero are potential vascular structures; we then calculated the number of pixels with a lower limit of k ranging from 0.01 to 5. Calculations were performed (1) in a window traced manually (Figure 2 B4) and focused on the ROI corresponding to the area of the biopsy by referring to the trail of the forceps (Figure 2 A1; Figure 2 B5 illustrates the area of the ROI with k values > 0.01); (2) on the full image; and (3) on the full image less the window.

Finally, the maximal value of k in the ROI (k_{max}) was also determined for each patient.

Statistical analysis. Correlations between histological and sonographic measures of the synovitis, as well as between these measures and the biological variables ESR and CRP, were determined by linear regression using the least-square method (Statview® 4.5; Abacus Concepts, Berkeley, CA,

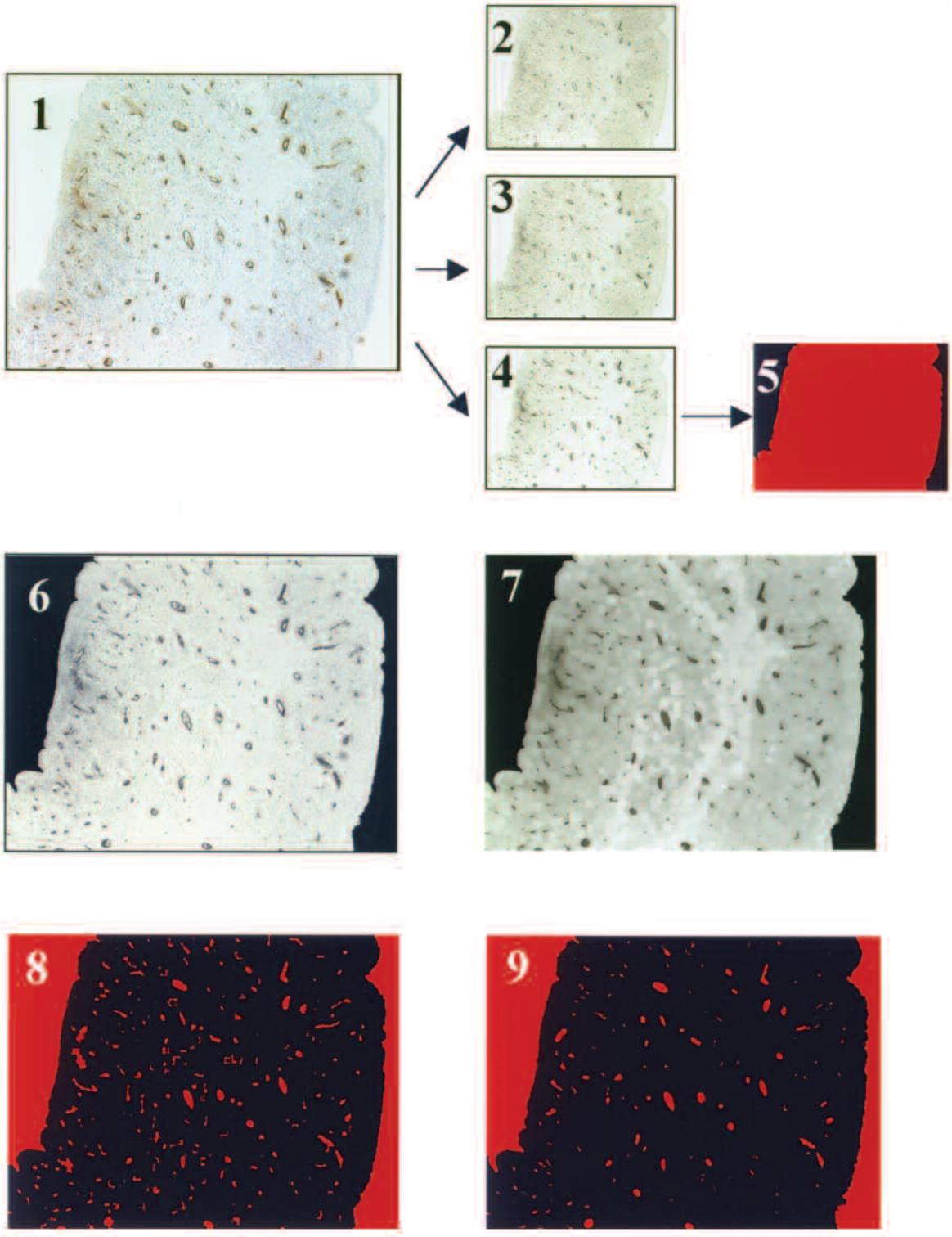

Figure 1. Image processing of histological sections: splitting of the colour image (1) into its red (2), green (3), and blue (4) components; a mask image (5) is used to isolate tissue area from the component background (6); (7) contrast enhancement of vessels; (8) transformation of the ROI into a binary image in which pixels that belong to vessels have the value 1 and those that belong to tissue the value 0; (9) final binary image in which small objects and artifacts were filtered.

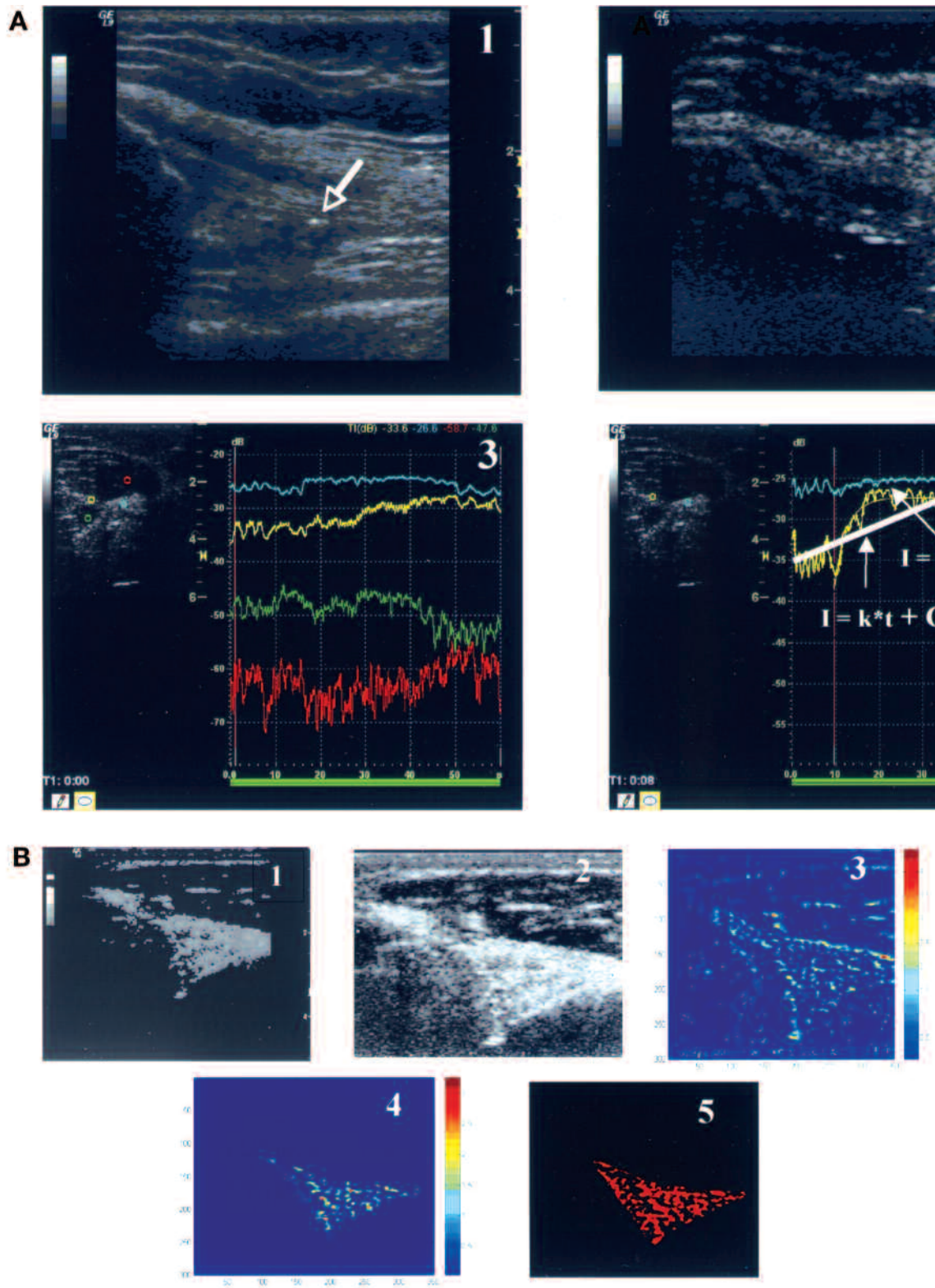

Figure 2. A. Synovitis sonography without and with microbubble contrast agent: (1) Image of the synovial region during biopsy; white arrow shows the trail of the biopsy forceps. (2) Contrast-enhanced coded phase-inversion harmonic sonography of the corresponding synovial region. (3 and 4) Time evolution of the gray-level intensity of ROI measured without (3) and with (4) a microbubble contrast agent injection. (4) Time evolution of the gray-level intensity fitted with a linear and an exponential function. B. Processing of US images: (1) Representative microbubble contrast image of the video stream; (2) image rescaled and framed to 400 x 400 pixels; (3) k image composed by pixels colored in function of their value; (4) window designed on the ROI allowing comparison of US measurements with the histological vessel density; (5) pixels in the window where k values are > 0.01.

USA) after logarithmic transformation. P values < 0.05 were considered significant.

RESULTS

Vessel density and k values. The vessel density of the 11 biopsies ranged from 1.4% to 7.7% (mean 4.3%; individual values shown in Table 1). We selected 3 representative vascular densities — low 2.0%, Patient 10), intermediate (4.1%, Patient 9), and high (7.7%, Patient 3) — and observed in the selected ROI 3 different profiles of distribution of the k values ($k > 0.01$; Figure 3). Synovitis with 2% density of vessels showed a reduced number of low k values ($k_{max} = 4.0$; Figure 3A). In synovitis with 4.1% of vessels, we observed more positive and higher k values ($k_{max} = 7.9$; Figure 3B). Synovitis with the highest histological density, 7.7% of vessels, showed both the highest number of positive k values and the highest values ($k_{max} = 13$; Figure 3C). In these 3 examples, the percentages of the ROI with k values > 0.01 were 42%, 46%, and 51%, respectively.

Individual k values > 0.01 in the ROI area ranged from 41% to 54% (Table 1), with a mean value of 46.6%.

A positive and linear significant correlation ($r = 0.93$, $p < 0.0001$) was found between the histological vessel density and the percentage of k values > 0.01 in the ROI area (Figure 4A). Of note, this significant correlation was lost when the k values were calculated on the whole image (400 × 400 pixels) including ($r = 0.07$, $p > 0.05$) or not including ($r = 0.06$, $p > 0.05$) the ROI (data not shown). The cutoff value of $k > 0.01$ gave the highest correlation between both variables, although correlations remained significant when other cutoff values were tested ($k > 0.05$, $r = 0.89$, $p < 0.001$; $k > 0.1$, $r = 0.78$, $p < 0.01$; $k > 0.15$, $r = 0.68$, $p < 0.05$; $k > 0.20$, $r = 0.61$, $p < 0.05$). Significance was lost for all higher cutoff values of k that were tested (0.25 to 5).

Because regions with the highest k values were those with the highest enhancement of echogenicity, i.e., regions whose probability to represent a vessel was maximal, we also calculated k_{max} values; k_{max} values ranged from 3.9 to 13.4 (mean 7.5; individual values shown in Table 1). Interestingly, a positive and linear significant correlation ($r = 0.79$, $p = 0.0037$) was also found between k_{max} values and the histological vessel densities (Figure 4B), as well as for k_{max} values and the percentage of $k > 0.01$ in the ROI area ($r = 0.72$, $p = 0.01$; data not shown).

Finally, the histological vessel density, the percentages of k values > 0.01 in the ROI area, and k_{max} values were also significantly correlated with log ESR and with log CRP (Table 2).

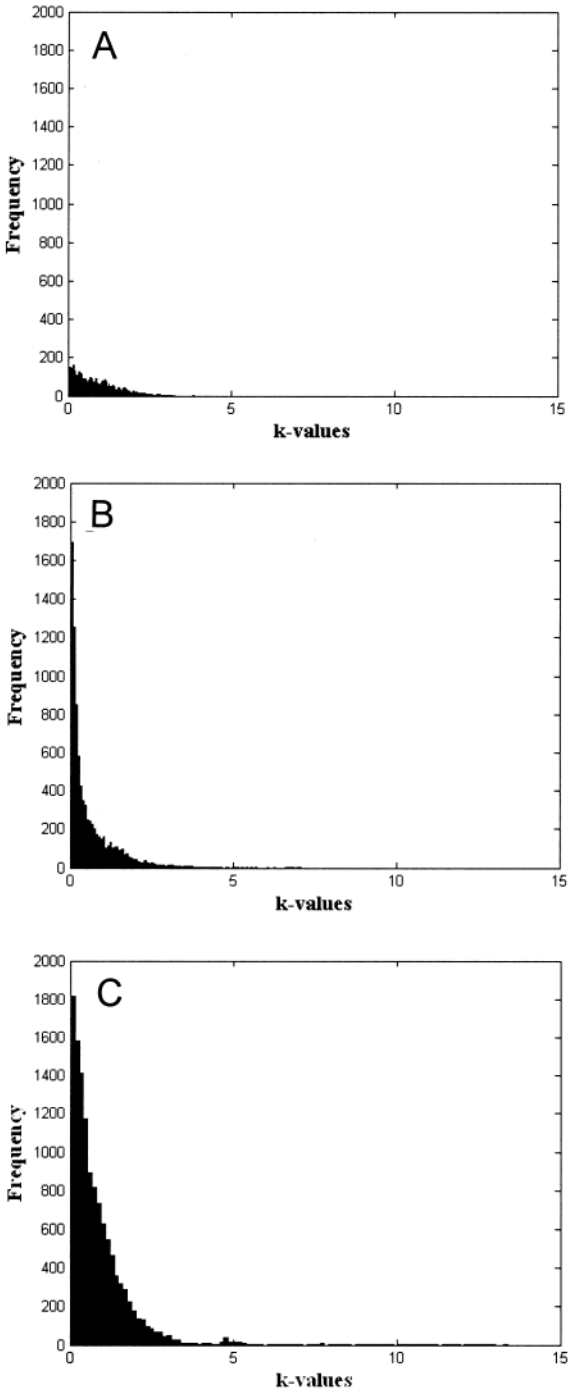

Figure 3. Histogram distribution of the k values > 0.01 in 3 representative histological vessel densities (percentage of the ROI): (A) low: 2.0%; (B) intermediate: 4.1%; (C) high: 7.7%.

DISCUSSION

The importance of angiogenesis in the onset and progression of RA as well as in the structural damage caused to adjacent cartilage and bone structures is unquestionable[7-9,13]. Visualization and quantification of vessels in RA synovitis are enabled by imaging techniques such as contrast-enhanced sonography in Doppler mode, and by highly sensitive color Doppler ultrasound techniques[47,48]. Despite enthusiastic reports[3,10,16-33], practical difficulties are encountered in separating artifacts from true Doppler signals[36-38].

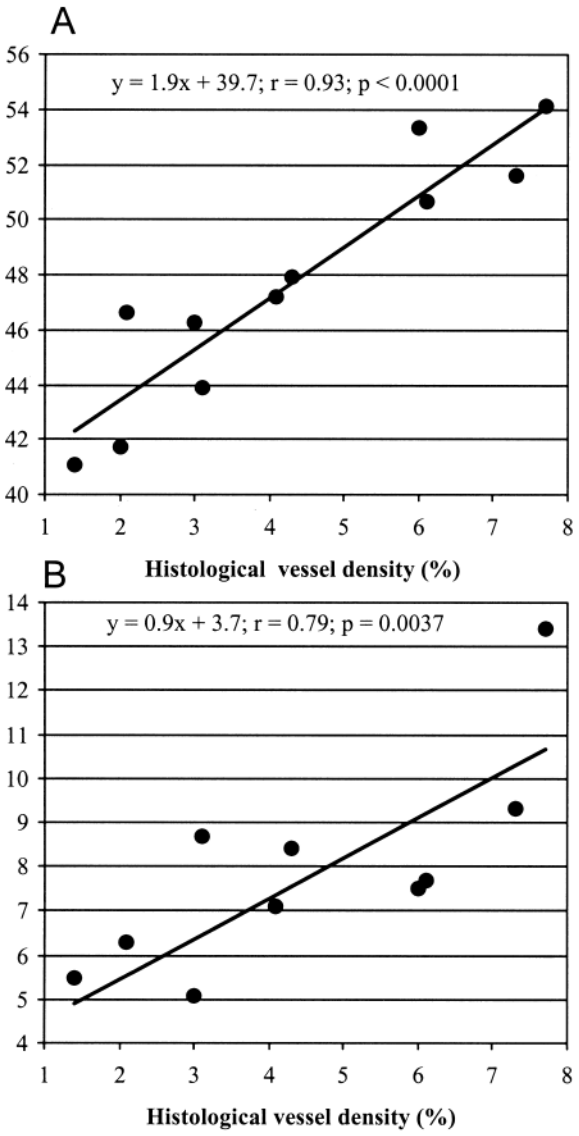

Figure 4. Correlations between histological vessel density and percentage of the ROI area with k values > 0.01 (A), and with k_{max} values in the ROI (B).

We propose an alternative methodology, B-mode contrast-enhanced CPI harmonic sonography, to study synovial vascularization. It is based on the fact that pixels with constant gray level during infusion of Sonovue® contrast medium show resting structures, whereas pixels that exhibit some acoustic enhancement where the microbubbles are moving are presumably the vessels. In the former, the k value, the slope of the equation [intensity (time) = k × time + C], is zero, and in the latter, k value is different from zero. It was shown that the synovial area with an increase of gray-level intensity during Sonovue® infusion (k > 0.01) was highly correlated with the vessel density measured on synovial biopsies performed in the same ROI. Further, both acoustic and histological quantifications could be fully automated.

Table 2. Significant correlations between histological/sonographic parameters of synovitis and 2 biological parameters of activity.

Parameters Tested	Log ESR		Log CRP	
	r	p	r	p
Histological vessel density	0.77	0.0054	0.69	0.0177
% of k > 0.01 in the ROI	0.87	0.0004	0.83	0.0015
k_{max}	0.67	0.0226	0.62	0.0418

ROI: region of interest; ESR: erythrocyte sedimentation rate; CRP: C-reactive protein.

Our results have shown that this technology is applicable to study the vascularization of synovitis, as previously shown for that of hepatocellular carcinoma or liver metastases[39,41]. The specificity of our results is based on the following arguments.

1. Correlation was obtained with the gold standard for vessel identification, immunohistology with Factor VIII staining[43].

2. Very close spatial and temporal relationships were respected between acoustic and arthroscopic procedures by a constant echographic control, reducing potential sample bias and probably improving the validity of the comparison.

3. The correlation found was restricted to the analysis of the acoustic ROI, which corresponds to the area where the biopsy was performed.

4. The correlation was conserved for several different thresholds of k values, which eliminate fortuitous findings. Further, acoustic and histological image quantifications were obtained with automated digital programs that support the reproducibility of the results.

Use of traditional methods of signal processing and mathematical morphology[44,45] enabled us to propose a method for quantifying the synovitis vascularization with an extreme sensitivity, as the best correlation between the acoustic enhancement and vessel density was obtained for k values as low as > 0.01. The results also convinced us retroactively of the validity of the processing options chosen: (1) analysis of all pixels present in the image or in the ROI instead of the restricted number of 6 allowed by the software supplied with the GE Logiq 9 US device; (2) transformation of the exponential equation fitting the gray-level enhancement given in the software into a linear one; and (3) automated extraction of every 100 images in the video loop to save 20 images selected for the final analysis. Determination of the maximal value of k (k_{max}) was an indication of how rapidly and intensely the gray level was enhanced during the infusion of the Sonovue® agent. It remains unknown whether high k_{max} values might indicate the presence of larger vessels or of vessels with higher flows, and conversely, k_{max} values were also significantly correlated with the histological vessel density. Correlation between the area of the ROI with k values > 0.01 and the

k_{max} values confirms close relationships whose significance remains to be determined.

By selecting patients with RA, PsA, and OA, we hoped to obtain a good range of vessel densities, and the range of 1.4% to 7.7% obtained appears to be satisfactory. For ethical reasons, arthroscopy was not performed in healthy volunteers who usually have no synovitis as shown in magnetic resonance imaging studies. The correlation with histological vessel density was obtained with enhanced acoustic areas ranging from 41.1% to 54.1% of the ROI. The strong difference in the scale of the histological and acoustic areas can be explained by the fact that histology yields a 2-dimensional image whereas US evaluation is a 3-dimensional vascular network projection onto a 2-dimensional image in a dynamic recording.

Elevated serum levels of ESR or CRP are classical indicators of persistence of the inflammatory process in diseased joints. The significant correlations we found between log ESR and log CRP and the 3 variables tested (histological vessel density, percentage of $k > 0.01$ in the ROI, and k_{max}) strongly support the clinical relevance of the methodology for studying joint vascularization. Among many publications, only 2 have found a correlation between joint Doppler sonography and the ESR[13] or serum CRP level[33]. Although it is not stated in the text, one can calculate from the data of Walther, *et al*[24] that serum CRP levels are significantly correlated with the quantitative vessel histological score ($n = 23$; $r = 0.51$, $p = 0.012$) but not with the power Doppler score ($n = 23$; $r = 0.41$, $p = 0.054$). Two recent studies[49,50] used contrast-enhanced (Sonovue®) gray-scale sonography. In the first[49], the contrast was used to improve detection of synovial vascularity, which improves characterization of intraarticular thickening, allowing differentiation between the active and non-active joints to increase from 60.1% to 97.3%. Further, thickness measurement in active RA synovitis was significantly increased. A time-intensity analysis[50] calculated the slope of the contrast-induced acoustic enhancement of synovitis in knee OA, with values graded on a semiquantitative scale according to the observation of no (0) or mild (1), medium (2), or strong (3) enhancement. This method allows quantification of digital synovial vascularization[50]. We observed with interest that this methodology is similar in its principles to what we developed, i.e., calculation of a slope (in our work the k value) during the acoustic enhancement induced by perfusion of Sonovue® medium. If the slope (k) value is zero, no vascularization is detected. A slope (k) value different from zero identifies vessels within the synovitis. An advantage of the US image processing we developed is that time-intensity analysis is calculated in each of the thousands of pixels that constitute the ROI, giving a global and automated result from an acoustically heterogeneous synovitis area. In other words, the question is no longer in which region must we calculate the slope, because calculation integrates the whole area.

Our work has several limitations. First, although hundreds of thousands of pixels were studied, they represent only 11 patients, and our data will have to be confirmed on a larger series. Second, the use of microbubble contrast agent increases the cost (about $80 per ampoule), with the time of the procedure restricted to one joint analysis during one perfusion that may generate side effects[4]. Yet the tolerance profile of the product is good[33,34], and no side effects occurred in our study, nor in others[49,50]. One more shortcoming is the loss of the noninvasive character of the US procedure[31,47]. For all these reasons, including the availability of new Doppler technologies, the interest in contrast-enhanced sonography in RA may be limited[31,47]. We agree with this, but only for application with the Doppler mode.

The methodology we have described could represent a valid alternative to the limitations of Doppler sonography. Contrast-enhanced gray-scale sonography is likely to transform vascular imaging to imaging of perfused tissue at the microvascular level[49]. A comparable approach using contrast-enhanced gray-scale US has been shown to adequately quantify intratumoral blood flow and monitor tissue vascular response to antiangiogenic therapy in mice[51]. A longitudinal study, after an anti-tumor necrosis factor-α treatment, for example, is needed to confirm the utility of the method for monitoring blood flow in synovitis.

Contrast-enhanced gray-scale sonography may represent a response to the hope that functional images obtained with color and power Doppler sonography corresponded to morphological findings obtained with real-time gray-scale sonography[37].

Acoustic enhancement after sulfur hexafluoride infusion, determined through automated digital quantifications, correlated with histological vessel density measurements of knee synovitis from patients with RA, OA, and PsA.

REFERENCES

1. Kane D, Balint PV, Sturrock RD. Ultrasonography is superior to clinical examination in the detection and localization of knee joint effusion in rheumatoid arthritis. J Rheumatol 2003;30:966-71.
2. Karim Z, Wakefield RJ, Quinn M, et al. Validation and reproducibility of ultrasonography in the detection of synovitis in the knee. A comparison with arthroscopy and clinical examination. Arthritis Rheum 2004;50:387-94.
3. Ribbens C, Andre B, Marcelis S, et al. Rheumatoid hand joint synovitis: gray-scale and power Doppler US quantifications following anti-tumor necrosis factor-α treatment: pilot study. Radiology 2003;229:562-9.
4. Ostergard M, Szkudlarek M. Imaging in rheumatoid arthritis — why MRI and ultrasonography can no longer be ignored. Scand J Rheumatol 2003;32:63-73.
5. Hauzeur JP, Mathy L, De Maertelaer V. Comparison between clinical evaluation and ultrasonography in detecting hydrarthrosis of the knee. J Rheumatol 1999;26:2681-3.
6. D'Agostino MA, Conaghan P, Le Bars M, et al. EULAR report on the use of ultrasonography in painful knee osteoarthritis. Part I. Prevalence of inflammation in osteoarthritis. Ann Rheum Dis 2005;64:1703-9.
7. FitzGerald O, Soden M, Yanni G, Robinson R, Breshnihan B.

Morphometric analysis of blood vessels in synovial membranes obtained from clinically affected and unaffected knee joints of patients with rheumatoid arthritis. Ann Rheum Dis 1991;50:792-6.
8. FitzGerald O, Bresnihan B. Synovial membrane cellularity and vascularity. Ann Rheum Dis 1995;54:511-5.
9. Paleolog EM. Angiogenesis in rheumatoid arthritis. Arthritis Res 2002;4 Suppl:S81-S90.
10. Hau M, Shultz H, Tony H-P, et al. Evaluation of pannus and vascularization of the metacarpophalangeal and proximal interphalangeal joints in rheumatoid arthritis by high-resolution ultrasound (multidimensional linear array). Arthritis Rheum 1999;42:2303-8.
11. Schmidt WA, Volker L, Zacher J, Schlafke M, Ruhnke M, Gromnica-Ihle E. Colour Doppler ultrasonography to detect pannus in knee joint synovitis. Clin Exp Rheumatol 2000;18:439-44.
12. Hau M, Kneitz C, Tony H-P, Keberle M, Jahans R, Jenett M. High resolution detects a decrease in pannus vascularization of small finger joints in patients with rheumatoid arthritis receiving treatment with soluble tumour necrosis factor α receptor (etanercept). Ann Rheum Dis 2002;61:55-8.
13. Klauser A, Frauscher F, Schirmer M, et al. The value of contrast-enhanced color Doppler ultrasound in the detection of vascularization of finger joints in patients with rheumatoid arthritis. Arthritis Rheum 2002;46:647-53.
14. Terslev L, Torp-Pedersen L, Savnik L, et al. Doppler ultrasound and magnetic resonance imaging of synovial inflammation of the hand in rheumatoid arthritis. A comparative study. Arthritis Rheum 2003;48:2434-41.
15. Terslev L, Torp-Pedersen S, Qvistgaard E, Danneskiold-Samsoe B, Bliddal H. Estimation of inflammation by Doppler ultrasound: quantitative changes after intra-articular treatment in rheumatoid arthritis. Ann Rheum Dis 2003;62:1049-53.
16. Qvistgaard E, Rogind H, Torp-Pedersen S, Terslev L, Danneskiold-Samsoe B, Bliddal H. Quantitative ultrasonography in rheumatoid arthritis: evaluation of inflammation by Doppler technique. Ann Rheum Dis 2001;60:690-3.
17. Newman JS, Adler RS, Bude RD, Rubin JM. Detection of soft-tissue hyperemia: value of power Doppler sonography. AJR Am J Roentgenol 1994;163:385-89.
18. Newman JS, Laing TJ, McCarthy CJ, Adler RS. Power Doppler sonography of synovitis: assessment of the therapeutic response — preliminary observations. Radiology 1996;198:582-84.
19. Martinoli C, Pretolesi F, Crespi G, et al. Power Doppler sonography: clinical applications. Eur J Radiol 1998;27 Suppl:S133-40.
20. Ferrell WR, Balint PV, Egan CG, Lockhart JC, Sturrick RD. Metacarpophalangeal joints in rheumatoid arthritis: laser Doppler imaging — initial experience. Radiology 2001;220:257-62.
21. Stone M, Bergin D, Whelan B, Maher M, Murray J, McCarthy C. Power Doppler ultrasound assessment of rheumatoid hand synovitis. J Rheumatol 2001;28:1979-82.
22. Giovagnorio F, Martinoli C, Coari G. Power Doppler sonography in knee arthritis — a pilot study. Rheumatol Int 2001;20:101-4.
23. Magarelli N, Guglielmi G, Di Matteo L, Tartaro A, Mattei PA, Bonomo L. Diagnostic utility of an echo-contrast agent in patients with synovitis using power Doppler ultrasound: a preliminary study with comparison to contrast-enhanced MRI. Eur Radiol 2001;11:1039-46.
24. Walther M, Harms H, Krenn V, Radke S, Faehndrich TP, Gohlke F. Correlation of power Doppler sonography with vascularity of the synovial tissue of the knee joint in patients with osteoarthritis and rheumatoid arthritis. Arthritis Rheum 2001;44:331-8.
25. Szkudlarek M, Court-Payen M, Strandberg C, Klarlund M, Klausen T, Østergaard M. Power Doppler ultrasonography for assessment of synovitis in the metacarpophalangeal joints of patients with rheumatoid arthritis: a comparison with dynamic resonance imaging. Arthritis Rheum 2001;44:2018-23.
26. Carotti M, Salam F, Manganelli P, Salera D, Simonetti B, Grassi W. Power Doppler sonography in the assessment of synovial tissue of the knee joint in rheumatoid arthritis: a preliminary experience. Ann Rheum Dis 2002;61:877-82.
27. Walther M, Harms H, Krenn V, Radke S, Kirschmer S, Gohkle F. Synovial tissue of the hip at power Doppler US: correlation between vascularity and power Doppler US signal. Radiology 2002;225:225-31.
28. Fiocco U, Ferro F, Cozzi L, et al. Contrast medium in power Doppler ultrasound for assessment of synovial vascularity: comparison with arthroscopy. J Rheumatol 2003;30:2170-6.
29. Szkudlarek M, Court-Paven M, Strandberg C, Klarlund M, Klausen T, Osterggard M. Contrast-enhanced power Doppler ultrasonography of the metacarpophalangeal joints in rheumatoid arthritis. Eur Radiol 2003;13:163-8.
30. Weidekamm C, Köller M, Weber M, Kainberger F. Diagnostic value of high-resolution B-mode and Doppler sonography for imaging of hand and finger joints in rheumatoid arthritis. Arthritis Rheum 2003;48:325-33.
31. Beckers C, Ribbens C, André B, et al. Assessment of disease activity in rheumatoid arthritis with 18F-FDG PET. J Nucl Med 2004;45:956-64.
32. Taylor PC, Steuer A, Gruber J, et al. Comparison of ultrasonographic assessment of synovitis and joint vascularity with radiographic evaluation in a randomized, placebo-controlled study of infliximab therapy in early rheumatoid arthritis. Arthritis Rheum 2004;50:1107-16.
33. Salaffi F, Carotti M, Manganelli P, Filippucci E, Giuseppetti GM, Grassi W. Contrast-enhanced power Doppler sonography of knee synovitis in rheumatoid arthritis: assessment of therapeutic response. Clin Rheumatol 2004;23:285-90.
34. Rees JD, Pilcher J, Heron C, Kiely PDW. A comparison of clinical vs ultrasound determined synovitis in rheumatoid arthritis utilizing gray-scale, power Doppler and the intravenous microbubble contrast agent "Sono-Vue". Rheumatology 2007;46:454-59.
35. Cardinal E, Lafortune M, Burns P. Power Doppler US in synovitis: reality or artifact? Radiology 1996;200:868-9.
36. Thiele R. Doppler ultrasonography in rheumatology: adding color to the picture. J Rheumatol 2008;35:8-10.
37. Balint PV, Mandl P, Kane D. "All that glistens is not gold" — Separating artefact from true Doppler signals in rheumatological ultrasound. Ann Rheum Dis 2008;67:141-2.
38. Torp-Pedersen ST, Terslev L. Settings and artifacts relevant in colour/power Doppler ultrasound in rheumatology. Ann Rheum Dis 2008;67:143-9.
39. Blomley MJK, Cooke JC, Unger EC, Monaghan MJ, Cosgrove DO. Microbubble contrast agents: a new era in ultrasound. BMJ 2001; 322:1222-5.
40. Bokor D. Diagnostic efficacy of SonoVue®. Am J Cardiol 2000;86:19G-24G.
41. Ding H, Kudo M, Onda H, et al. Evaluation of posttreatment response of hepatocellular carcinoma with contrast-enhanced coded phase-inversion harmonic US: comparison with dynamic CT. Radiology 2001;221:721-30.
42. Bokor D, Chambers JB, Rees PJ, Mant TG, Luzzani F, Spinazzi A. Clinical safety of Sonovue®, a new contrast agent for ultrasound imaging, in healthy volunteers and in patients with chronic obstructive pulmonary disease. Invest Radiol 2001;36:104-9.
43. Sehested M, Hou-Jensen K. Factor VIII-related antigen as an endothelial cell marker in benign and malignant diseases. Virch Arch (Path Anat) 1981;391:217-25.
44. Soille P. Morphological image analysis: principles and applications. Berlin: Springer; 1999:104-10.
45. Kapur JN, Sahoo PK, Wong AKC. A new method for gray-level

picture thresholding using the entropy of the histogram. Computer Vision, Graphics and Image Processing 1985;29:273-85.
46. Sahoo PK, Soltani S, Wong AKC. A survey of thresholding techniques. Computer Vision, Graphics, and Image Processing 1988;41:233-60.
47. Terslev L, Torp-Pedersen S, Bang N, Koenig MJ, Nielsen MB, Bliddal H. Doppler ultrasound findings in healthy wrists and finger joints before and after use of two different contrast agents. Ann Rheum Dis 2005;64:824-7.
48. Terslev L, von der Recke P, Torp-Pedersen S, Koenig MJ, Nielsen MB, Bliddal H. Diagnostic sensitivity and specificity of Doppler ultrasound in rheumatoid arthritis. J Rheumatol 2008;35:49-53.
49. Klauser A, Demharter J, De Marchi A, et al. Contrast enhanced gray-scale sonography in assessment of joint vascularity in rheumatoid arthritis: results from the IACUS Study Group. Eur Radiol 2005;15:2404-10.
50. Song IH, Burmester GR, Backhaus M, et al. Knee osteoarthritis. Efficacy of a new method of contrast-enhanced musculoskeletal ultrasonography in detection of synovitis in patients with knee osteoarthritis in comparison with magnetic resonance imaging. Ann Rheum Dis 2008;67:9-25.
51. McCarville MB, Streck CJ, Dickson PV, Li CS, Nathwani AC, Davidoff AM. Angiogenesis initiators in a murine neuroblastoma model: quantitative assessment of intratumoral blood flow with contrast-enhanced gray-scale US. Radiology 2006;240:73-81.